Electronic Supplementary Material (ESI) for Soft Matter.

Supporting Information for

MoS_2 nanosheets induced destructive alterations in *Escherichia coli* bacterial membrane

Monika Kumari and Hemant K. Kashyap*

Department of Chemistry, Indian Institute of Technology Delhi, Hauz Khas, New Delhi 110016, India

E-mail: hkashyap@chemistry.iitd.ac.in

Phone: +91-(0)11-26591518. Fax: +91-(0)11-26581102

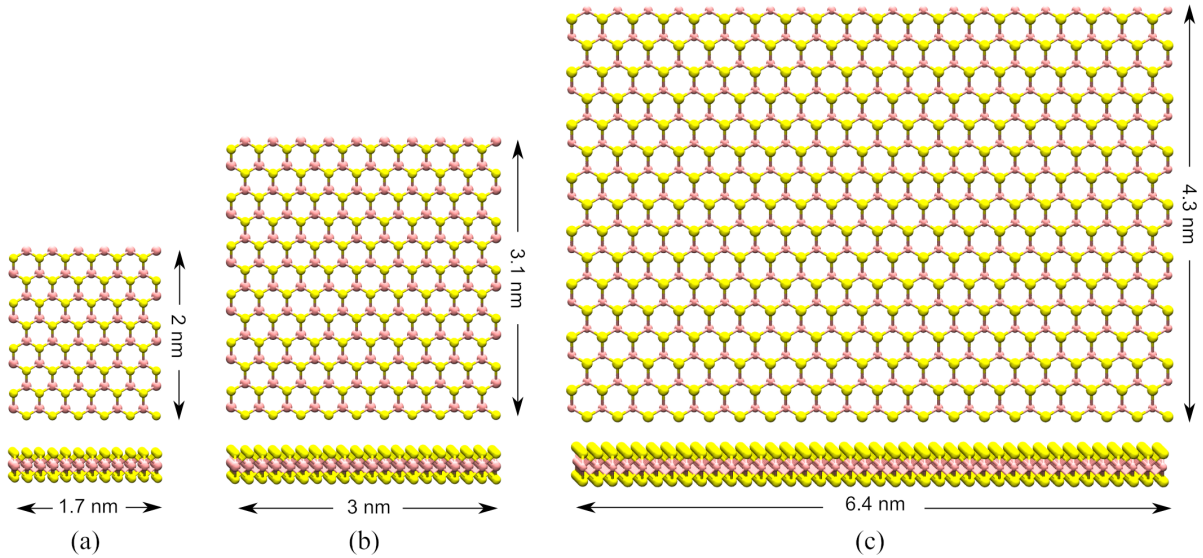

Figure S1: The top-view (upper panels) and lateral-view (lower panels) of the MoS_2 nanosheets used in this study, (a) 2 nm × 1.7 nm, (b) 3.1 nm × 3 nm, (c) 6.4 nm × 4.3 nm. The Mo and S atoms are displayed as pink and yellow spheres, respectively.

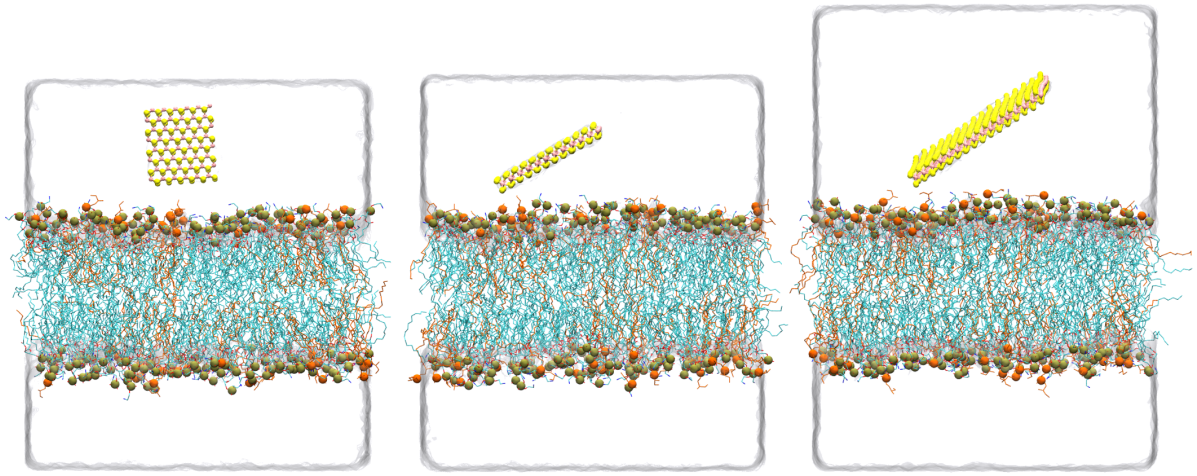

Figure S2: Initial simulation setup of (a) S22, (b) S33, and (c) S64 systems. The representation of MoS_2 nanosheets are kept same as Fig. S1. The DOPE and DOPG lipids are shown in cyan and orange sticks with their head P highlighted in tan and orange colored beads, respectively. Water boundaries are represented by grey surfaces. Ions are omitted for clarity.

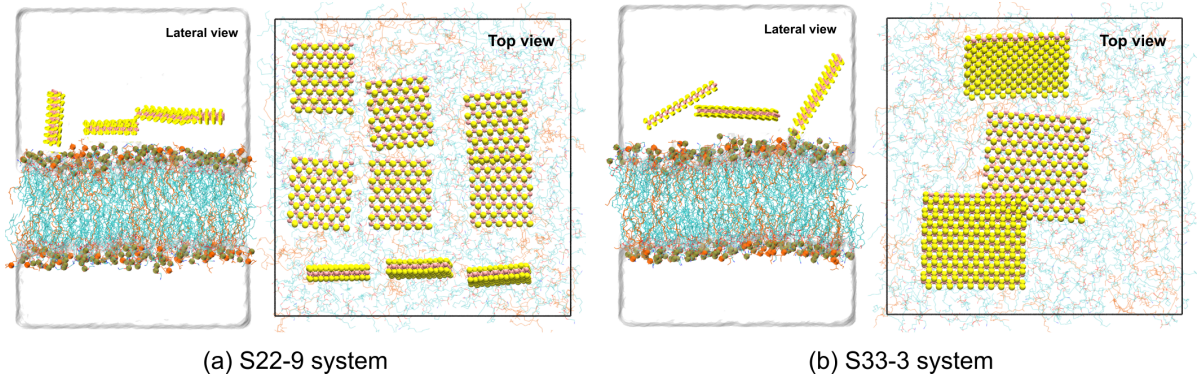

Figure S3: Initial simulation setup (lateral and top views) of (a) S22-9, and (b) S33-3 systems. The representation scheme is kept same as Fig. S2.

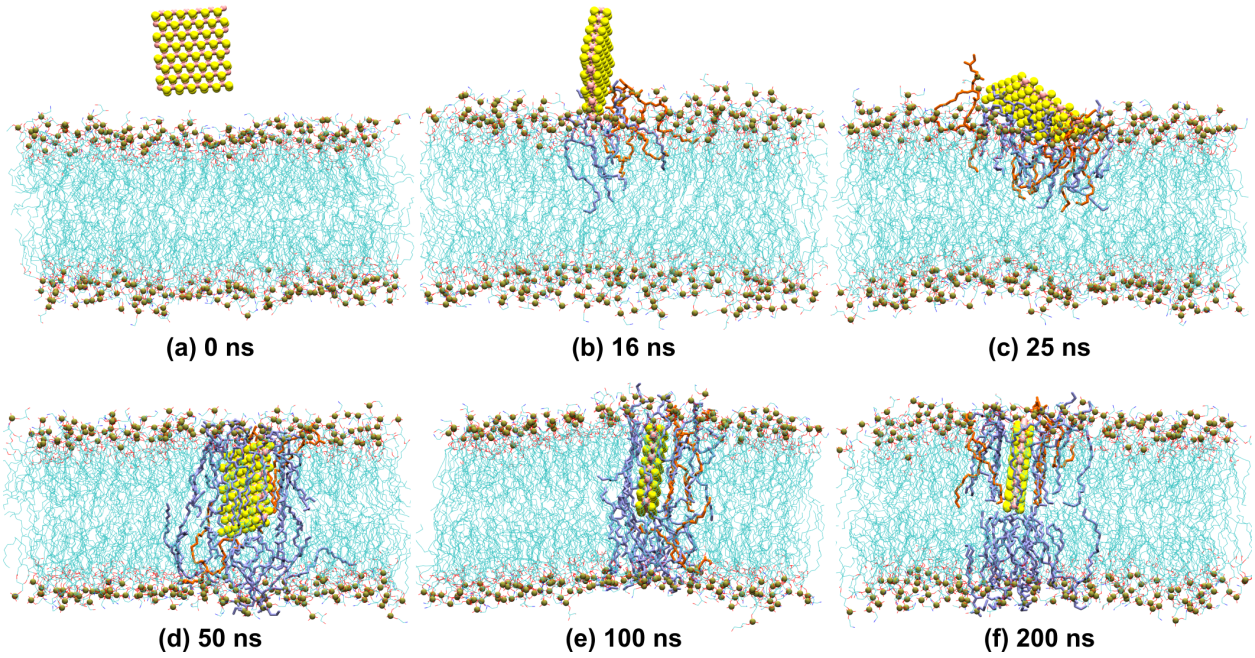

Figure S4: Trajectory snapshots of S22 system displaying the various steps of MoS_2 nanosheet interaction with bacterial membrane with time. The membrane lipid tails are represented in cyan color with their head phosphorus atoms highlighted in tan colored beads. MoS_2 sheet is shown in ball and stick representation with Mo and S colored as pink and yellow, respectively. The DOPE and DOPG lipids in the vicinity of MoS_2 sheet are shown as iceblue and orange sticks, respectively. Subfigures b-c show the step I i.e. surface interaction and lipid extraction and subfigures d-f represent MoS_2 penetration in bilayer core region (step II).

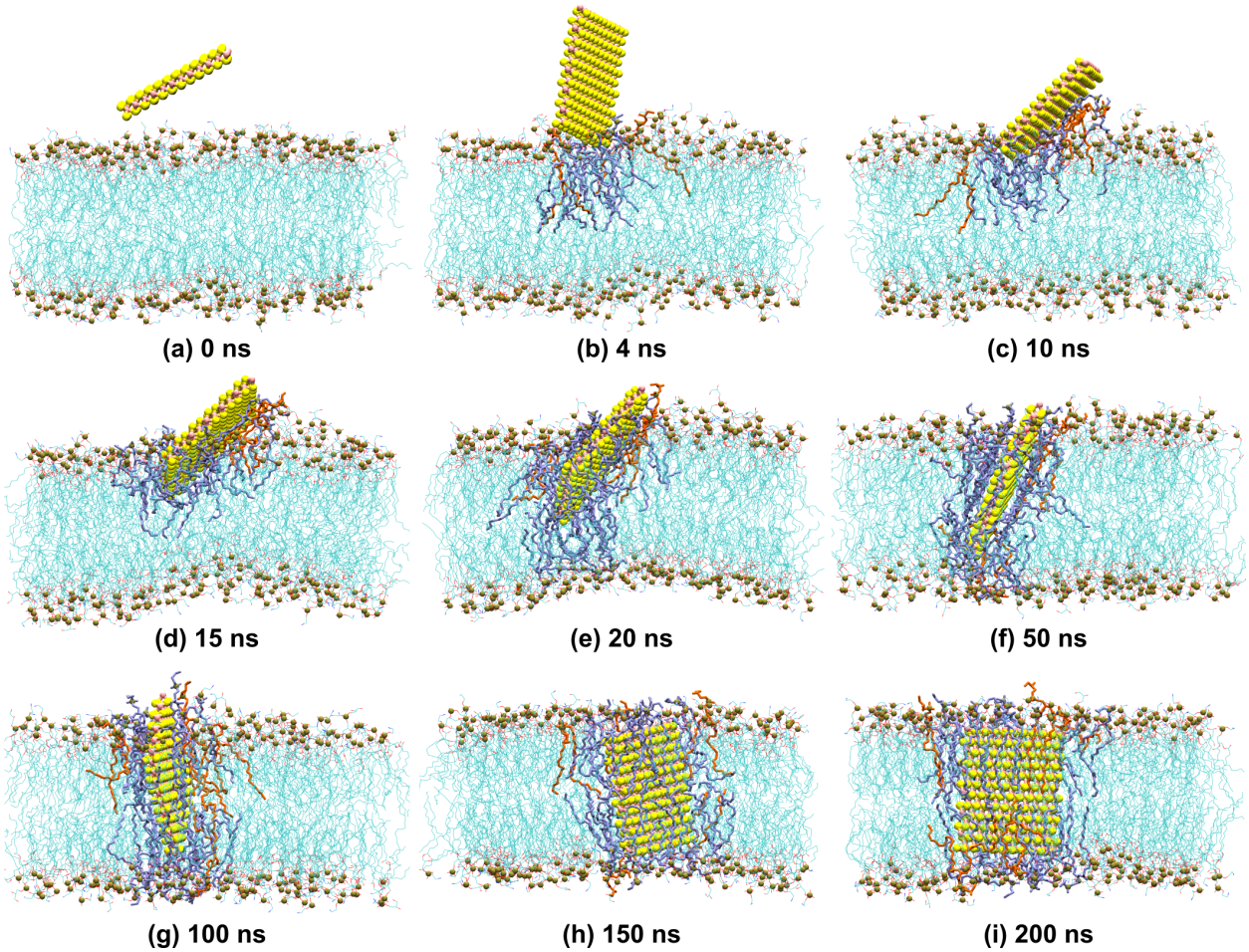

Figure S5: Trajectory snapshots of S33 system displaying the various steps of MoS_2 sheet insertion in bacterial membrane with time. The representation scheme is same as followed in Fig. S4. Subfigures b-e show the step I i.e. surface interaction and lipid extraction and subfigures f-i represent MoS_2 penetration (step II).

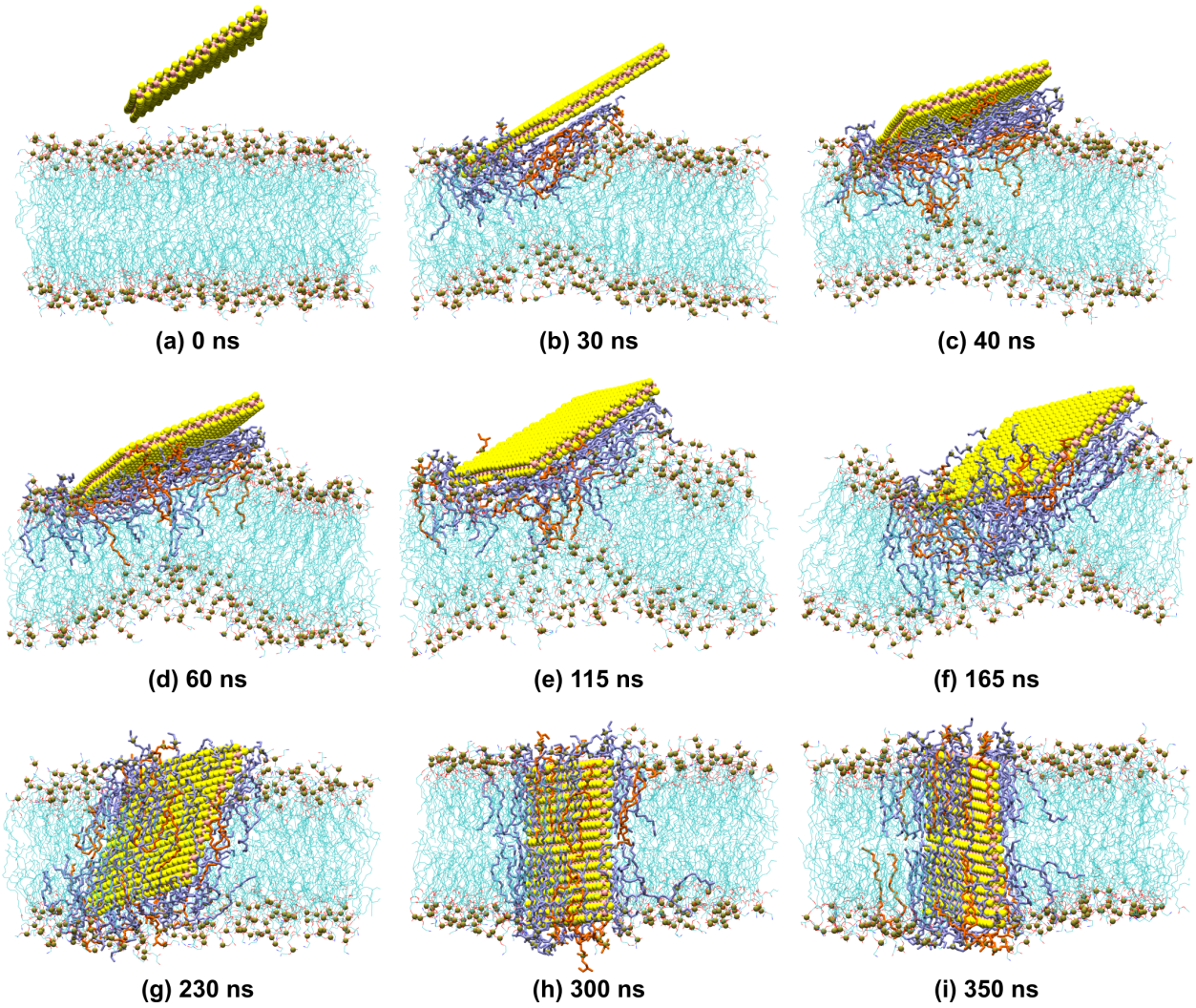

Figure S6: Trajectory snapshots of S64 system displaying the various steps of MoS_2 sheet interactions with bacterial membrane with time. The display settings are kept same as Fig. S4. Subfigures b-f show the step I i.e. surface interaction and lipid extraction and subfigures g-i represent MoS_2 penetration (step II).

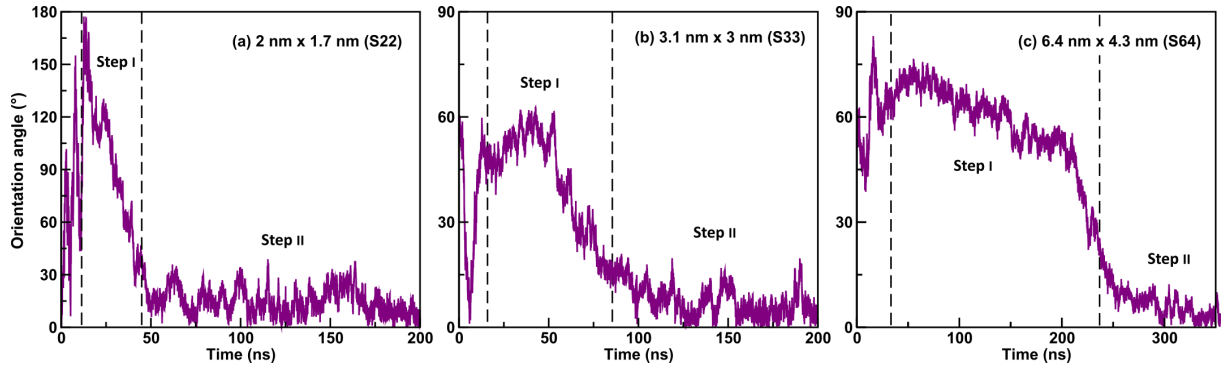

Figure S7: Time-dependent evolution of MoS_2 nanosheet orientation with respect to membrane normal (z-axis). Note that after complete insertion, the nanosheets orient nearly parallel to z-axis with orientation angle approximately equal to 0°.

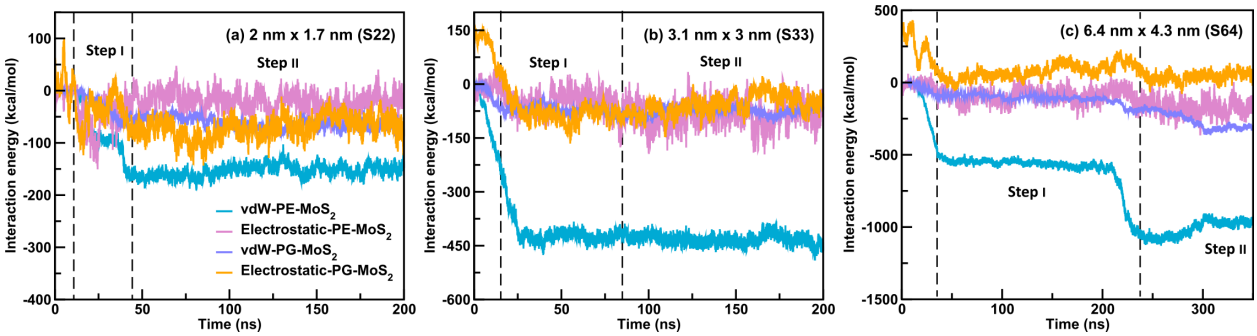

Figure S8: The interaction energy of PE and PG lipids with MoS_2 nanosheet. There occurs sharp decrease in van der Waals interaction energy as more and more lipids come in contact with the nanosheet; first dip at surface contact and spontaneous lipid extraction and second during insertion in the membrane.

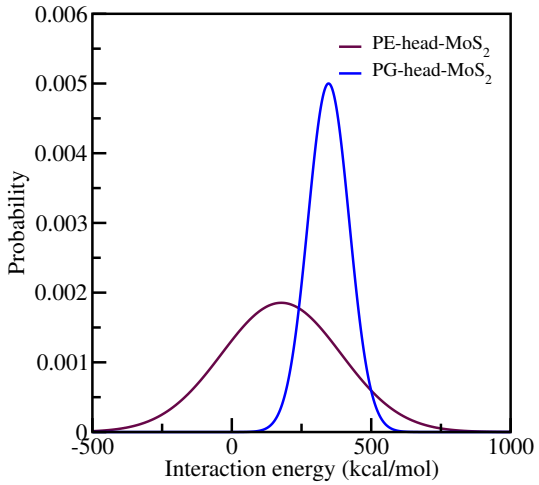

Figure S9: Total interaction energy for PE and PG lipid head groups with MoS_2 nanosheet in S64 system.

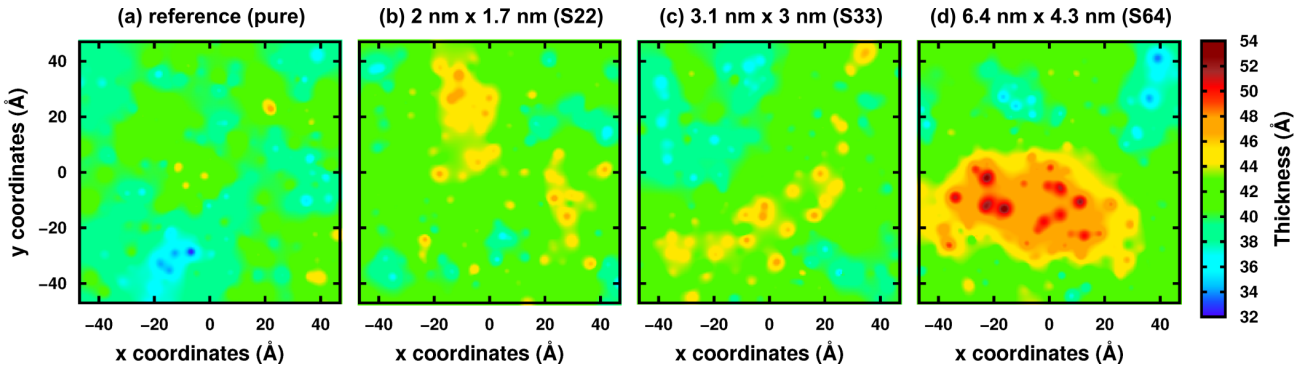

Figure S10: Variation in bilayer thicknessmap in presence of different MoS_2 nanosheets with respect to the pure *E. coli* bilayer. S64 system shows exceptional rise in thickness around the nanosheet penetration site.

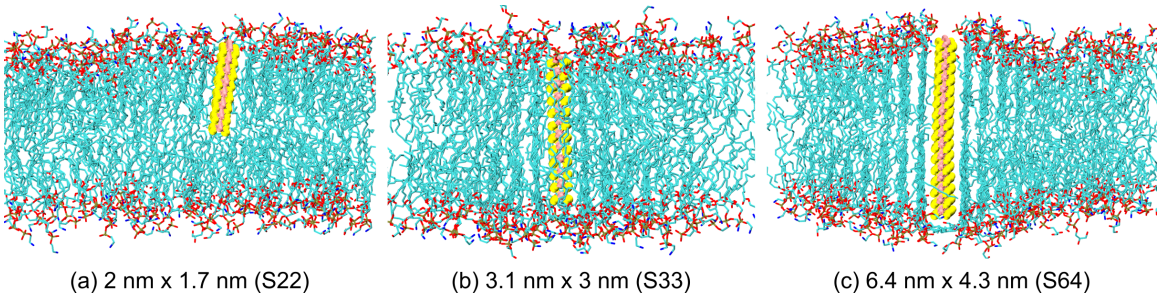

Figure S11: Representative snapshots displaying the layerwise arrangement of lipid molecules around inserted MoS_2 nanosheets. The layers become more and more defined with increasing size of the nanosheet.

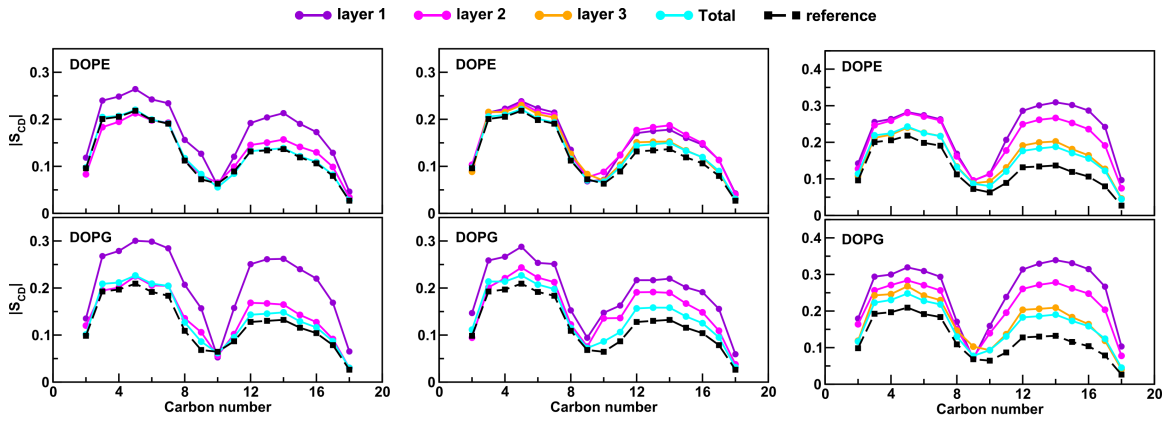

(a) (b) (c)

Figure S12: Layer-wise and total orientation order parameter of ths $sn2$ tails of PE and PG lipids of (a) S22, (b) S33, and (c) S64 systems. The "reference" data represents the order parameter of pure bilayer in absence of any nanosheet. Since the S22 system does not have a well-defined 3rd layer, the data is reported for first two layers for this system.

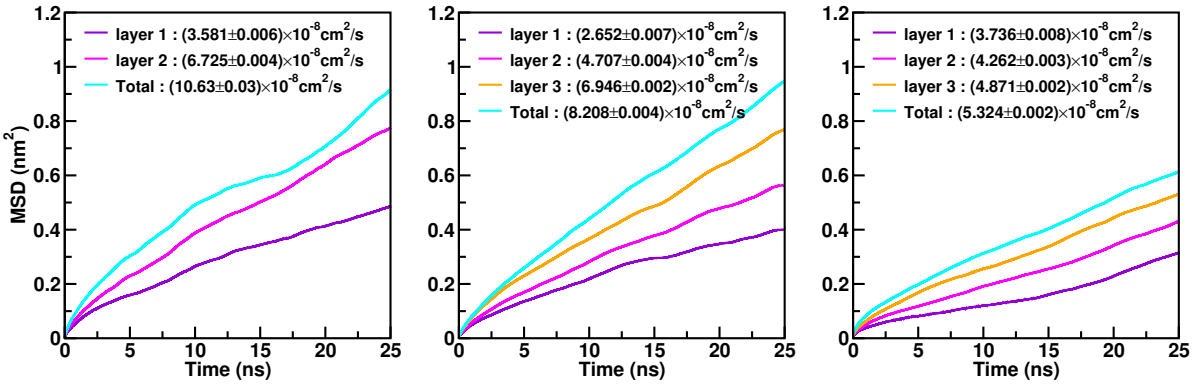

(a) (b) (c)

Figure S13: Lateral mean square displacement (MSD) of lipids present in binding layers and compared with averaged total for (a) S22, (b) S33, and (c) S64 systems.

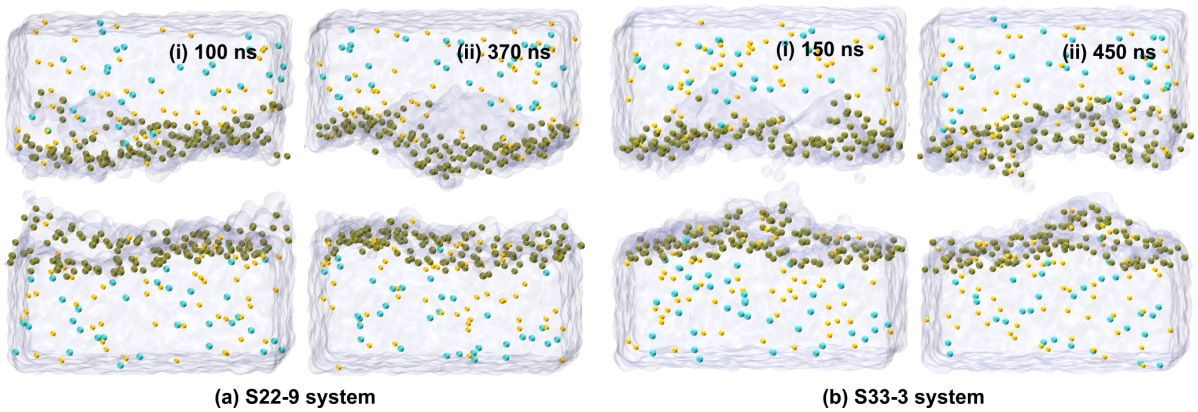

Figure S14: Trajectory snapshots showing considerable water intrusion in lipid hydrophobic region of bacterial membrane in presence of multiple (a) 2 nm × 1.7 nm sized nanosheets (S22-9) and (b) 3.1 nm × 3 nm sized nanosheets (S33-3). Two snapshots are shown per system at (i) representative time frame where the nanosheets are mostly interacting at the surface while (ii) represents the last frame. Water molecules are shown in transparent surf representation with Na^+ and Cl^- ions rendered as golden and cyan spheres, respectively. Lipid head phosphorus atoms are shown as tan beads. Lipid tails and MoS_2 nanosheets are omitted for clarity.